

Random forest–based out-of-distribution detection for robust lung cancer auto-segmentation

Aneesh Rangnekar and Harini Veeraraghavan

Department of Medical Physics, Memorial Sloan Kettering Cancer Center, New York, USA

ABSTRACT

Accurate detection and segmentation of cancerous lesions from computed tomography (CT) scans is essential for automated treatment planning and cancer treatment response assessment. Transformer-based models with self-supervised pretraining have achieved strong performance on in-distribution (ID) data but often generalize poorly on out-of-distribution (OOD) inputs. We investigate this behavior for lung cancer segmentation using an encoder–decoder model. Our encoder is a Swin Transformer pretrained with masked image modeling (SimMIM) on 10,432 unlabeled 3D CT scans spanning cancerous and non-cancerous conditions, and the decoder was randomly initialized. This model was evaluated on an independent ID test set and four OOD scenarios: chest CT cohorts (pulmonary embolism and negative COVID-19) and abdomen CT cohorts (kidney cancers and non-cancerous pancreas). OOD detection was performed at the scan level using RF-Deep, a random forest classifier applied to contextual tumor-anchored feature representations. We evaluated 920 3D CTs (172,650 images) and observed that RF-Deep achieved FPR95s of 18.26% and 27.66% on the chest CT cohorts, and near-perfect detection ($< 0.1\%$ FPR95) on abdomen-CT cohorts, consistently outperforming established OOD methods. These results demonstrate that our RF-Deep classifier provides a simple, lightweight and effective approach for enhancing the reliability of segmentation models in clinical deployment.

Keywords: Swin Transformer, auto-segmentation, lung cancer, out-of-distribution

1. PURPOSE

Among deep learning architectures, models that combine pretrained transformer backbones with convolutional decoders have demonstrated high accuracies in volumetric auto-segmentation of organs and tumors from 3D radiological scans.^{1–6} A major challenge in deploying these models at scale is the potential accuracy degradation when applied to real-world scenarios that differ from those seen during training. For example, models trained to segment malignant lung cancers from chest CTs may also encounter scans that have benign nodules from lung cancer screening or scans containing unrelated diseases such as pulmonary embolisms, producing unanticipated and incorrect results outside their intended scope.

Traditional segmentation metrics such as the Dice similarity coefficient (DSC) and Hausdorff distance at 95th percentile (HD95) are designed to assess performance on in-distribution (ID) datasets, but are insufficient indicators of models’ robustness to out-of-distribution (OOD) data. OOD detection methods relying on model confidence scores, such as MaxSoftmax,⁷ often fail in scenarios where models produce confidently incorrect segmentations.^{8–10} Alternative approaches using secondary models like VQ-GANs^{11,12} require large training data, are computationally intensive, and lack interpretability, limiting their practical utility in high-throughput clinical workflows. Radiomics feature-based methods^{13,14} have shown to be effective at distinguishing scans of organs but have not generalized yet to tumors. To address these limitations, we propose RF-Deep, a lightweight scan-level OOD detection framework that leverages tumor-anchored contextual features from backbone encoders for reliable clinical deployment.

We evaluated our approach on far-OOD scans (diseases in different anatomic sites) and challenging near-OOD scans (different diseases in the same site with similar appearance). Our contributions are:

Send correspondence to Aneesh Rangnekar (Email: rangnea@mskcc.org)

- i. a lightweight, model-agnostic OOD detection framework using random forest on deep feature representations extracted from the segmentation model’s encoder. While random forests for OOD detection are established, our contribution lies in the task-anchored application, a practical deployment concern under-explored in medical imaging,
- ii. demonstration on lung cancer segmentation including near-ODD (pulmonary embolism, COVID-19) and far-ODD (kidney cancers, healthy pancreas) scenarios, and
- iii. a systematic comparison against established OOD detection methods using five public datasets comprising 172,650 images from 920 patient scans.

2. METHOD

2.1 OOD detection task definition

Let \mathcal{D}_{in} denote the distribution of lung cancer CT scans, closely matching the lung CT data used to fine-tune our segmentation model, and \mathcal{D}_{out} represents the scans that differ in pathology and anatomy. Our objective is to determine whether a new scan x belongs to \mathcal{D}_{in} or \mathcal{D}_{out} , at the scan level. We compute voxel-level metric scores, average them to obtain $S(x)$, and apply a decision threshold τ : scans with $S \leq \tau$ are flagged as ID, and $S \geq \tau$ as OOD. Since tumor segmentation is binary, aggregation is restricted to the predicted tumor regions, leveraging model-relevant spatial context while excluding irrelevant anatomy.

2.2 Segmentation model architecture

Our segmentation model is a hybrid transformer-convolution architecture that combines the global contextual modeling of a hierarchical Swin Transformer¹⁵ encoder with the local spatial precision of a U-Net-based¹⁶ convolutional decoder to accurately delineate anatomical boundaries of tumors. The encoder uses a depth configuration of 2-2-12-2 across four stages with $4 \times 4 \times 4$ patch size, enabling multi-scale feature aggregation, while windowed self-attention reduces computational complexity yet preserves global context for large volumetric inputs ($128 \times 128 \times 128$ voxels). The decoder was randomly initialized, whereas the encoder was pretrained using SimMIM,¹⁷ a self-supervised masked image modeling approach in which 75% of 3D patches are masked and reconstructed. This strategy leverages large-scale unlabeled CT data to learn robust, anatomy-aware feature representations^{2, 18-20} and provides a strong foundation for downstream tumor segmentation and OOD detection.

2.3 OOD Detection with RF-Deep

Patient scans exhibit high variability and unlike natural images, may span the large anatomical boundaries, making a global OOD assessment inefficient. We therefore focus on the most semantically relevant areas, the tumor regions predicted by the segmentation model. Our approach (Fig. 1) can be outlined in four steps: (i) fine-tune a segmentation model with pretrained backbone encoders for lung tumor segmentation, (ii) extract tumor-anchored 3D crops and multi-scale encoder features, (iii) aggregate features into fixed-length representation maintaining global context focused on clinically relevant tumor regions and train a random forest classifier (RF-Deep) with ID and OOD examples, and (iv) classify new scans as ID or OOD using the trained RF-Deep. Critically, RF-Deep adds negligible computational cost as the feature extraction stage leverages the already-stored encoder representations from segmentation, and random forest inference is orders of magnitude faster than running secondary deep models.

2.4 Implementation details

Datasets. We fine-tuned the model on NSCLC Radiomics²¹ (N=317), with LRAD²² (N=140) as the ID dataset. OOD evaluation used RSNA-Pulmonary Embolism²³ (N=120), *negative* COVID-19 MIDRC²⁴ (N=120), KiTS-23²⁵ (N=120), and Pancreas-CT²⁶ (N=82), totaling 920 scans. **Segmentation.** All models were implemented using PyTorch²⁷ and MONAI,²⁸ fine-tuned using cross-entropy and Dice loss with a batch size of 16 across 4 NVIDIA GPUs. We used a learning rate of 2×10^{-4} , with linear warm-up and cosine annealing over 1000 epochs. Augmentations included flips, rotations, affine, and intensity shifts. Inputs were normalized (HU $[-400, 400]$), resampled (1mm^3), and cropped to 128^3 . Sliding window with 50% overlap was used for inference. **RF-Deep.** Random forest (1000 trees, max depth 20, balanced weights) via the scikit-learn library. Features were extracted from 8 tumor-anchored crops per scan, and predictions were averaged at inference. **Comparative approaches.**

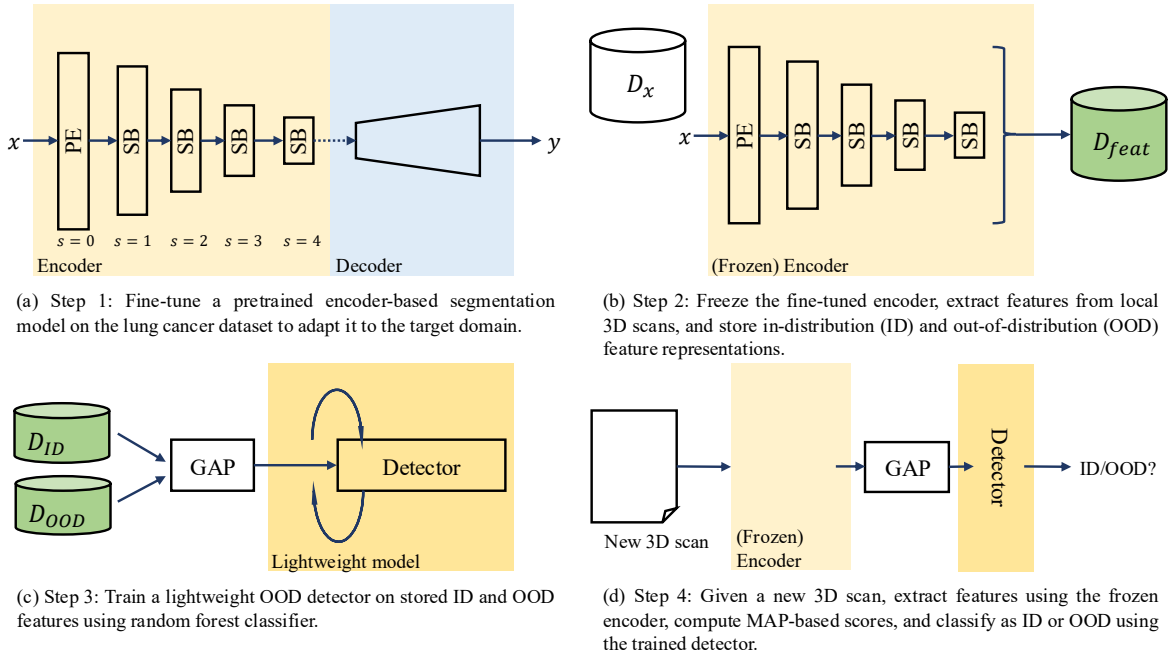


Figure 1: High-level pipeline of the proposed out-of-distribution (OOD) detection framework, focusing on segmentation for lung cancer CT scans. After fine-tuning, the encoder is frozen, and features are extracted from the patch embedding (PE) layer and Swin blocks (SB) across all four stages to be used with a random forest classifier.

Table 1: Out-of-distribution (OOD) detection performance across different OOD detection strategies for our segmentation model. Results are reported as AUROC (\uparrow) and FPR95 (\downarrow), with best values per dataset highlighted in bold.

Method	Pulmonary embolism		COVID-19		Kidney cancer		Pancreas	
	AUROC	FPR95 (%)	AUROC	FPR95 (%)	AUROC	FPR95 (%)	AUROC	FPR95 (%)
MaxSoftmax	88.74	37.01	89.53	53.25	96.72	12.34	97.26	14.29
MaxLogits	90.88	34.42	91.30	37.01	97.51	7.140	98.12	6.490
Energy	90.97	35.06	91.05	37.01	97.50	7.140	98.12	6.490
Entropy	90.59	33.81	92.47	53.24	96.97	12.23	97.55	12.95
RF-Radiomics	88.26	40.13	90.98	36.36	95.94	19.87	95.90	15.06
RF-Deep (Ours)	95.16	18.26	92.88	27.66	99.81	0.110	99.89	0.720

RF-Radiomics used 293 IBSI-compliant features²⁹ via PyCERR,^{30,31} reduced with recursive elimination, and with same config as RF-Deep. We also evaluated MaxSoftmax,⁷ MaxLogits,³² energy,³³ and entropy. **OOD experiment protocol.** RF-based approaches used a fixed 40/60 patient-level train-test split, repeated over 100 matched seeds to assess stability. Other baselines used the full cohorts as they require no auxiliary data. **Evaluation metrics.** We report AUROC and FPR95 (%) to measure ID-OOD separability.^{34,35}

3. RESULTS

Our results demonstrate that RF-Deep provides robust scan-level OOD detection for lung cancer segmentation, outperforming established approaches including MaxSoftmax and MaxLogits (1). Encoder features from the SimMIM-pretrained and fine-tuned model, paired with RF, consistently yielded higher AUROC and lower FPR95 across all scenarios, with large margin gains in the abdominal cohorts (FPR95 \leq 0.1, second best is 6 points away). The substantial performance differences, particularly in far-OOD scenarios, reflect the advantage of task-relevant contextual features over confidence-based heuristics. Fig. 2 visually shows RF-Deep’s ability to detect scans from completely different anatomical sites and different disease cases, with some limitations. In pulmonary

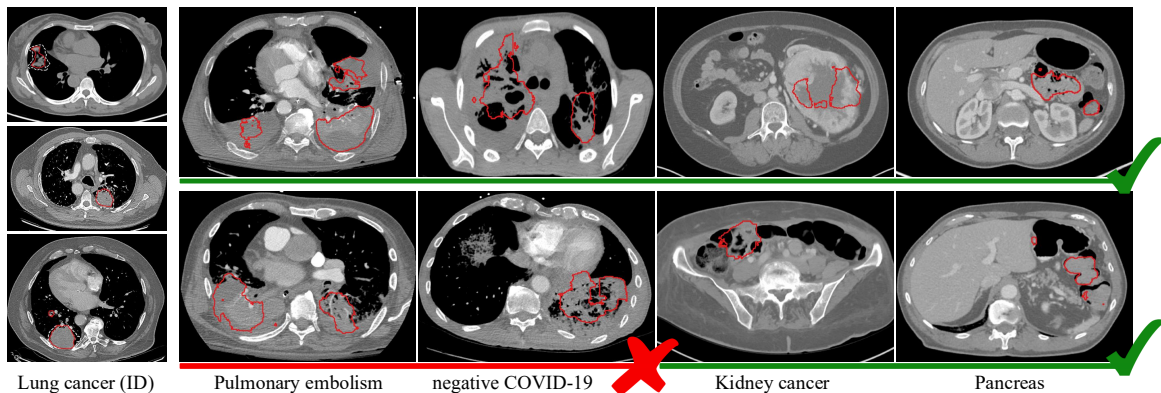


Figure 2: Representative results with green checkmarks indicating correctly detected OOD scans and the red cross highlighting missed cases. The red contours denote segmentations from the model, illustrating that naive confidence measures may fail when tumor-like structures exist in non-cancer cohorts.

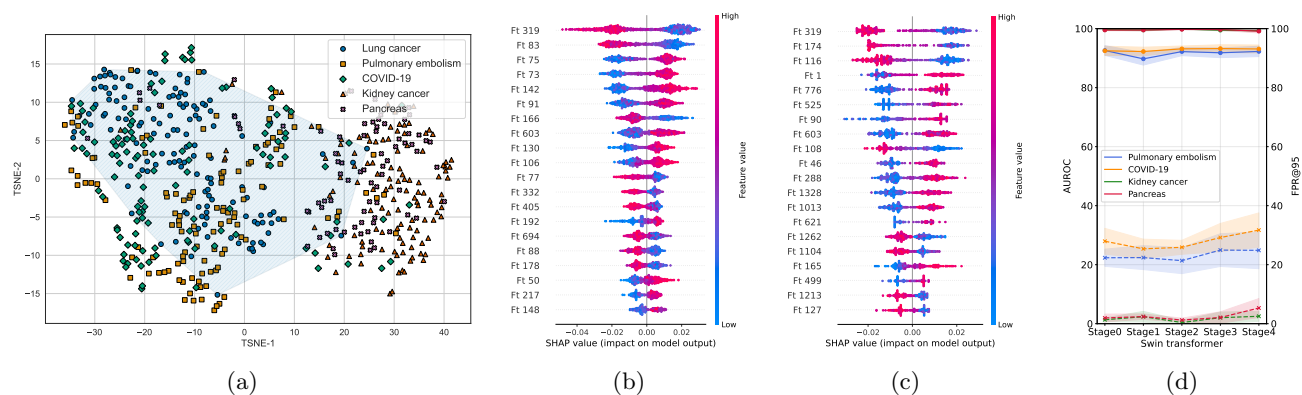


Figure 3: Supporting analyses of our approach: (a) t-SNE visualization shows ID/OOD separation in encoder representations (the convex hull denotes extent of ID), (b,c) SHAP analysis highlighting feature importance and interpretability in RSNA-Pulmonary Embolism and KiTS-23 kidney cancer datasets respectively, and (d) Stage-wise ablation shows individual RF-Deep performance from Swin Transformer encoder features.

embolism cases, we observed that the segmentation model often highlights tumor-like structures rather than the emboli; nevertheless, our contextual features enable RF-Deep to correctly classify these scans as OOD in most cases, surpassing non-contextual approaches. Additionally, we computed an unsupervised clustering of the features³⁶ across all cohorts (Fig. 3a) and observed semi-clear, distinct clusters for in-distribution (ID) and OOD cohorts, making them separable with the random forest classifier. Fig. 3b and Fig. 3c show the SHAP analysis on the RF-Deep providing interpretability and identifying which encoder features are most influential in classifying a scan as OOD, allowing for future work into feature reduction. Finally, stage-wise ablation (Fig. 3d), wherein only features corresponding to a particular stage of the transformer were used for training RF-Deep, demonstrated that mid- and early-deep level Swin Transformer features are most effective, aligning with our SHAP findings.

4. CONCLUSION

We performed a comprehensive evaluation of different OOD detection methods applied to the clinical task of lung cancer segmentation. Our analysis showed that, even though segmentation models can predict tumors incorrectly at times, RF-Deep, built on encoder features from our fine-tuned model with a random forest, consistently outperforms established methods. The approach is lightweight, interpretable, and improves the reliability of segmentation in both near- and far-OOD clinical scenarios. Future work involves scaling to more disease sites, understanding multi-class behavior, and evaluating generalization across other backbone pretraining strategies.

ACKNOWLEDGMENTS

This research was partially supported by NCI R01CA258821 and Memorial Sloan Kettering (MSK) Cancer Center Support Grant/Core Grant NCI P30CA008748.

REFERENCES

- [1] Willemink, M., Roth, R., and Sandfort, V., “Toward foundational deep learning models for medical imaging in the new era of transformer networks,” *Radiol Artif Intell* **4**(6) (2022).
- [2] Jiang, J., Tyagi, N., Tringale, K., Crane, C., and Veeraraghavan, H., “Self-supervised 3d anatomy segmentation using self-distilled masked image transformer (SMIT),” in [*International Conference on Medical Image Computing and Computer-Assisted Intervention*], 556–566, Springer (2022).
- [3] Nguyen, D. M. H., Nguyen, H., Mai, T. T. N., Cao, T., Nguyen, B. T., Ho, N., Swoboda, P., Albarqouni, S., Xie, P., and Sonntag, D., “Joint self-supervised image-volume representation learning with intra-inter contrastive clustering,” in [*Proc. 37th AAAI*], AAAI Press (2023).
- [4] Yan, X., Naushad, J., Sun, S., Han, K., Tang, H., Kong, D., Ma, H., You, C., and Xie, X., “Representation recovering for self-supervised pre-training on medical images,” in [*2023 IEEE/CVF Winter Conference on Applications of Computer Vision (WACV)*], 2684–2694 (2023).
- [5] Qayyum, A., Razzak, I., Mazher, M., Khan, T., Ding, W., and Niederer, S., “Two-stage self-supervised contrastive learning aided transformer for real-time medical image segmentation,” *IEEE Journal of Biomedical and Health Informatics*, 1–10 (2023).
- [6] Gu, H., Dong, H., Yang, J., and Mazurowski, M. A., “How to build the best medical image segmentation algorithm using foundation models: a comprehensive empirical study with segment anything model,” *arXiv preprint arXiv:2404.09957* (2024).
- [7] Hendrycks, D. and Gimpel, K., “A baseline for detecting misclassified and out-of-distribution examples in neural networks,” *Proceedings of International Conference on Learning Representations* (2017).
- [8] Yeung, M., Rundo, L., Nan, Y., Sala, E., Schönlieb, C.-B., and Yang, G., “Calibrating the dice loss to handle neural network overconfidence for biomedical image segmentation,” *Journal of Digital Imaging* **36**(2), 739–752 (2023).
- [9] Hendrycks, D., Basart, S., Mazeika, M., Zou, A., Kwon, J., Mostajabi, M., Steinhardt, J., and Song, D., “Scaling out-of-distribution detection for real-world settings,” *ICML* (2022).
- [10] Zimmerer, D., Full, P. M., Isensee, F., Jäger, P., Adler, T., Petersen, J., Köhler, G., Ross, T., Reinke, A., Kascenas, A., et al., “Mood 2020: A public benchmark for out-of-distribution detection and localization on medical images,” *IEEE Transactions on Medical Imaging* **41**(10), 2728–2738 (2022).
- [11] Graham, M. S., Tudosiu, P.-D., Wright, P., Pinaya, W. H. L., Jean-Marie, U., Mah, Y. H., Teo, J. T., Jager, R., Werring, D., Nachev, P., et al., “Transformer-based out-of-distribution detection for clinically safe segmentation,” in [*International Conference on Medical Imaging with Deep Learning*], 457–476, PMLR (2022).
- [12] Pinaya, W. H., Tudosiu, P.-D., Gray, R., Rees, G., Nachev, P., Ourselin, S., and Cardoso, M. J., “Unsupervised brain imaging 3d anomaly detection and segmentation with transformers,” *Medical Image Analysis* **79**, 102475 (2022).
- [13] Vasiliuk, A., Frolova, D., Belyaev, M., and Shirokikh, B., “Limitations of out-of-distribution detection in 3d medical image segmentation,” *Journal of Imaging* **9**(9), 191 (2023).
- [14] Konz, N., Chen, Y., Gu, H., Dong, H., Chen, Y., and Mazurowski, M. A., “Rad: A metric for medical image distribution comparison in out-of-domain detection and other applications,” (2024).
- [15] Liu, Z., Lin, Y., Cao, Y., Hu, H., Wei, Y., Zhang, Z., Lin, S., and Guo, B., “Swin transformer: Hierarchical vision transformer using shifted windows,” in [*Proceedings of the IEEE/CVF international conference on computer vision*], 10012–10022 (2021).
- [16] Ronneberger, O., Fischer, P., and Brox, T., “U-net: Convolutional networks for biomedical image segmentation,” in [*International Conference on Medical Image Computing and Computer-Assisted Intervention*], 234–241, Springer (2015).

- [17] Xie, Z., Zhang, Z., Cao, Y., Lin, Y., Bao, J., Yao, Z., Dai, Q., and Hu, H., “Simmmim: A simple framework for masked image modeling,” in [*Proceedings of the IEEE/CVF conference on computer vision and pattern recognition*], 9653–9663 (2022).
- [18] Hatamizadeh, A., Nath, V., Tang, Y., Yang, D., Roth, H. R., and Xu, D., “Swin unetr: Swin transformers for semantic segmentation of brain tumors in mri images,” in [*Brainlesion: Glioma, Multiple Sclerosis, Stroke and Traumatic Brain Injuries*], 272–284, Springer International Publishing, Cham (2022).
- [19] Tang, Y., Yang, D., Li, W., Roth, H. R., Landman, B., Xu, D., Nath, V., and Hatamizadeh, A., “Self-supervised pre-training of swin transformers for 3d medical image analysis,” in [*Proceedings of the IEEE/CVF Conference on Computer Vision and Pattern Recognition*], 20730–20740 (2022).
- [20] Jiang, J., Rangnekar, A., and Veeraraghavan, H., “Self-supervised learning improves robustness of deep learning lung tumor segmentation models to ct imaging differences,” *Medical Physics* (Dec. 2024).
- [21] Aerts, H., Velazquez, E. R., Leijenaar, R., Parmar, C., Grossmann, P., Cavalho, S., Bussink, J., Monshouwer, R., Haibe-Kains, B., Rietveld, D., et al., “Data from nslc-radiomics,” *The cancer imaging archive* (2015).
- [22] Bakr, S., Gevaert, O., Echegaray, S., Ayers, K., Zhou, M., Shafiq, M., Zheng, H., Zhang, W., Leung, A., Kadoch, M., et al., “Data for nslc radiogenomics collection,” *The Cancer Imaging Archive* **10**, K9 (2017).
- [23] Colak, E., Kitamura, F. C., Hobbs, S. B., Wu, C. C., Lungren, M. P., Prevedello, L. M., Kalpathy-Cramer, J., Ball, R. L., Shih, G., Stein, A., et al., “The rsna pulmonary embolism ct dataset,” *Radiology: Artificial Intelligence* **3**(2), e200254 (2021).
- [24] Tsai, E. B., Simpson, S., Lungren, M. P., Hershman, M., Roshkovan, L., Colak, E., Erickson, B. J., Shih, G., Stein, A., Kalpathy-Cramer, J., Shen, J., Hafez, M. A., John, S., Rajiah, P., Pogatchnik, B. P., Mongan, J. T., Altinmakas, E., Ranschaert, E., Kitamura, F. C., Topff, L., Moy, L., Kanne, J. P., and Wu, C., “Medical imaging data resource center (MIDRC) - RSNA international COVID open research database (RICORD) release 1b - chest ct covid-,” (2021).
- [25] Heller, N., Isensee, F., Trofimova, D., Tejpaul, R., Zhao, Z., Chen, H., Wang, L., Golts, A., Khapun, D., Shats, D., Shoshan, Y., Gilboa-Solomon, F., George, Y., Yang, X., Zhang, J., Zhang, J., Xia, Y., Wu, M., Liu, Z., Walczak, E., McSweeney, S., Vasdev, R., Hornung, C., Solaiman, R., Schoepfoerster, J., Abernathy, B., Wu, D., Abdulkadir, S., Byun, B., Spriggs, J., Struyk, G., Austin, A., Simpson, B., Hagstrom, M., Virnig, S., French, J., Venkatesh, N., Chan, S., Moore, K., Jacobsen, A., Austin, S., Austin, M., Regmi, S., Papanikolopoulos, N., and Weight, C., “The KiTS21 challenge: Automatic segmentation of kidneys, renal tumors, and renal cysts in corticomedullary-phase ct,” (2023).
- [26] Roth, H. R., Lu, L., Farag, A., Shin, H.-C., Liu, J., Turkbey, E. B., and Summers, R. M., “Deeporgan: Multi-level deep convolutional networks for automated pancreas segmentation,” in [*Medical Image Computing and Computer-Assisted Intervention—MICCAI 2015: 18th International Conference, Munich, Germany, October 5-9, 2015, Proceedings, Part I 18*], 556–564, Springer (2015).
- [27] Paszke, A., Gross, S., Massa, F., Lerer, A., Bradbury, J., Chanan, G., Killeen, T., Lin, Z., Gimelshein, N., Antiga, L., et al., “Pytorch: An imperative style, high-performance deep learning library,” *Advances in neural information processing systems* **32** (2019).
- [28] Cardoso, M. J., Li, W., Brown, R., Ma, N., Kerfoot, E., Wang, Y., Murrey, B., Myronenko, A., Zhao, C., Yang, D., et al., “Monai: An open-source framework for deep learning in healthcare,” *arXiv preprint arXiv:2211.02701* (2022).
- [29] Zwanenburg, A., Vallières, M., Abdalah, M. A., Aerts, H. J., Andrearczyk, V., Apte, A., Ashrafinia, S., Bakas, S., Beukinga, R. J., Boellaard, R., et al., “The image biomarker standardization initiative: standardized quantitative radiomics for high-throughput image-based phenotyping,” *Radiology* **295**(2), 328–338 (2020).
- [30] Deasy, J. O., Blanco, A. I., and Clark, V. H., “CERR: a computational environment for radiotherapy research,” *Medical physics* **30**(5), 979–985 (2003).
- [31] Apte, A. P., Iyer, A., Crispin-Ortuzar, M., Pandya, R., Van Dijk, L. V., Spezi, E., Thor, M., Um, H., Veeraraghavan, H., Oh, J. H., et al., “Extension of CERR for computational radiomics: A comprehensive MATLAB platform for reproducible radiomics research,” *Medical physics* **45**(8), 3713–3720 (2018).
- [32] Hendrycks, D., Basart, S., Mazeika, M., Zou, A., Mostajabi, M., Steinhardt, J., and Song, D. X., “Scaling out-of-distribution detection for real-world settings,” in [*International Conference on Machine Learning*], (2022).

- [33] Liu, W., Wang, X., Owens, J., and Li, Y., “Energy-based out-of-distribution detection,” *Advances in neural information processing systems* **33**, 21464–21475 (2020).
- [34] Davis, J. and Goadrich, M., “The relationship between precision-recall and roc curves,” in [*Proceedings of the 23rd international conference on Machine learning*], 233–240 (2006).
- [35] Liang, S., Li, Y., and Srikant, R., “Enhancing the reliability of out-of-distribution image detection in neural networks,” *arXiv preprint arXiv:1706.02690* (2017).
- [36] Masarczyk, W., Ostaszewski, M., Imani, E., Pascanu, R., Miłoś, P., and Trzcinski, T., “The tunnel effect: Building data representations in deep neural networks,” *Advances in Neural Information Processing Systems* **36** (2024).